Analytical and Bioanalytical Chemistry (2019) 411:4277–4292
https://doi.org/10.1007/s00216-019-01620-9

TRENDS

Recent trends in analysis of nanoparticles in biological matrices

Zuzana Gajdosechova[1] · Zoltan Mester[1]

Received: 12 November 2018 / Revised: 21 December 2018 / Accepted: 16 January 2019 / Published online: 14 February 2019

Abstract

The need to assess the human and environmental risks of nanoparticles (NPs) has prompted an adaptation of existing techniques and the development of new ones. Nanoparticle analysis poses a great challenge as the analytical information has to consider both physical (e.g. size and shape) and chemical (e.g. elemental composition) state of the analyte. Furthermore, one has to contemplate the transformation of NPs during the sample preparation and provide sufficient information about the new species derived from such alteration. Traditional techniques commonly used for NP analysis such as microscopy and light scattering are still frequently used for NPs in simple matrices; however, they have limitations in the analysis of complex environmental and biological samples. On the other hand, recent improvements in data acquisition frequencies and reduction of settling time of ICP-MS brought inorganic mass spectrometry into the forefront of NPs analysis. However, with the increasing demand of analytical information related to NPs, emerging techniques such as enhanced darkfield hyperspectral imaging, nano-SIMS and mass cytometry are in their way to fill the gaps. This trend review presents and discusses the state-of-the-art analytical techniques and sample preparation methods for NP analysis in biological matrices.

Keywords Nanoparticle analysis · Nano-SIMS · Cy-TOF · Biological tissue · Single-particle ICP-MS

Introduction

The class of nano-size materials is very large and diverse as it includes nano-films and coatings (one dimension < 100 nm), nanotubes and wires (two dimensions < 100 nm) and nanoparticles (NPs, three dimensions < 100 nm) [1]. Nano-size materials can occur in the environment as a result of bioformation (HgSe NPs in tissues of marine mammals), be produced unintentionally (black carbon NPs as a result of combustion), be intentionally produced although not meant to be released to the environment (Ag NPs in food packaging) or be intentionally produced for specific environmental and biomedical applications (nanoscale motors [2, 3]). Due to their unique physiochemical and electronic properties, nano-sized materials have found applications in a variety of commercial sectors from medicine to aerospace engineering. Engineered NPs have been synthesised from metals, non-metals, bioceramics and polymeric materials and once released to the environment NPs can undergo a number of physical and chemical transformations. They can form reversible agglomerates or stable large aggregates. On the other hand, some metal-containing NPs such as silver and zinc oxides can undergo dissolution and release ionic species.

As a consequence of their size, NPs exhibit very different physiochemical properties compared to their respective bulk materials. These include changes in thermal conductivity, solubility, catalytic or optical properties. The change in surface-to-volume/mass ratio is thought to have the most significant influence on their altered behaviour [4]. As the size of the particles decreases, the proportion of atoms at the particle surface increases, and thus, the surface properties generally dictate the behaviour of NPs.

With an increasing abundance and variety of NPs found in the environment, their uncontrolled release is starting to raise concerns that the very same properties that make NPs desirable may also pose a threat to the environment and human health. Nanoparticles can relatively easily enter the human body and transverse biological barriers reaching sensitive

Published in the topical collection *Young Investigators in (Bio-)Analytical Chemistry* with guest editors Erin Baker, Kerstin Leopold, Francesco Ricci, and Wei Wang.

✉ Zuzana Gajdosechova
Zuzana.Gajdosechova@nrc.ca

[1] NRC Metrology, 1200 Montreal Road, Ottawa, ON K1A0R6, Canada

organs. A plethora of recent studies has focused on the toxicity of NPs at varying concentrations; however, characterisation of NPs is often done in water suspensions or culture-free growth media. While these data are important, they are not necessarily representative of true NP behaviour ihin the living organism. A recent review of in vitro and in vivo studies investigating the interaction of NPs in chemical mixtures concluded that the impacts are far more complex and it is not possible to clearly identify either positive or negative effects, further confounding risk-benefit estimations of NPs [5]. In recent years, the number of publications concerning NPs in animal and human tissues has risen significantly and they are starting to re-shape the understanding of NPs in the context of their everyday use and promoting regional legislations. For instance, the EU Commission adapted a reporting metrics and requires that analytical techniques provide particle number concentration rather than a mass concentration [6]. Indeed, a small mass fraction of NPs may contain a large number of very small NPs, which possess higher reactivity and can more easily breach biological barriers. Similarly, it was acknowledged by the European Food Safety Agency (EFSA) that TiO_2 NPs, common food additive in chewing gums, candies or toothpastes, also known as E171, is to a small extent absorbed after oral application and distributed to various organs [7]. And although it is difficult to predict the course of nano-science, the broad range of NP applications is indicative of the long-term use of nano-technologies. Therefore, it is necessary to carry out risk and safety assessment studies, develop reliable analytical methods to measure NPs and introduce appropriate safety regulations for workers, consumers and the environment.

Occupational exposure limits (OELs) are widely recognised as essential tools for regulating workers' exposure to harmful chemicals and cover more than 6000 substances. However, there are no specific regulatory OELs addressing exposure to nanoscale materials [8]. The main setback is due to a lack of toxicity data from long-term animal inhalation and epidemiological studies. However, worldwide efforts had been seen to address and regulate production and safe use of nano-size materials either through new legislations or non-binding recommendations/international standards. As there is no specific legislation dedicated solely to nano-size materials, they fall under existing legislations depending on their type or purpose of their use. For example, TiO_2 added to food products for technological purposes or to improve solubility, flavour or bioavailability is governed by the EU in the "Food Improvement Agent Package" which includes a wide number of regulations [9]. Existing legislations are viewed as sufficient and specific enough to regulate nano-size materials, although some amendments, such as internationally harmonised approach concerning nano-size material marketing and their safe use, have been suggested. A comprehensive in-depth review of regulatory aspects of nanotechnology has been recently published by Amenta et al. [9].

The objective of this article is to identify the most recent trends and developments in NP analysis with special focus on the analysis of NPs in biological tissue. The pre-selection was based on a thorough literature search limited to the past 5 years of publications with some exceptions. While some publications were found to be particularly interesting, the authors regret any inadvertent omission of reference to relevant papers. It is out of the scope of this trend article to provide a comprehensive literature review; however, the readers are directed to relevant review articles if more detailed information is desired.

Analytical techniques for NP characterisation with focus on biological matrices

With an increasing demand for the development of specialised NPs, advanced analytical techniques and instrumentation have been and continue to be developed to provide suitable tools for their characterisation. A graphic summary of discussed analytical techniques can be found in Fig. 1.

Electron and optical microscopy

Electron microscopy has a long track record in the characterisation of NPs in an array of matrices. Due to its capability to visualise the NPs and thus obtain information about their size, shape, state of the aggregation, electron microscopy is considered to be one of the most powerful techniques for NP analysis [10, 11]. Transmission electron microscopes (TEM) provide spatial resolution below 1 nm, which can be matched by scanning electron microscopes (SEM) fitted with a field-emission electron gun. However, the true power of microscopy lies in possibilities of their coupling with different spectroscopic tools which provide elemental and structural information of NPs. Using high-resolution field-emission gun scanning electron microscopy in combination with X-ray analysis (FEG-SEM/EDX), Makama et al. were able to identify the chemical composition of engineered NPs taken up by earthworms from contaminated soil [12]. Correlation between observed size and shape of the particles found in the tissue with primary particles present in the soil confirmed that the primary particles were transported across the biological membrane. In another study, TEM equipped with EDX was used for analysis of chemical composition and shape of Se NPs found in Se-rich yeast [13]. This information was subsequently used for single-particle analysis using inductively coupled plasma mass spectrometry (ICP-MS) which requires pre-existing knowledge of the shape and density of particles for accurate sizing of unknown particles.

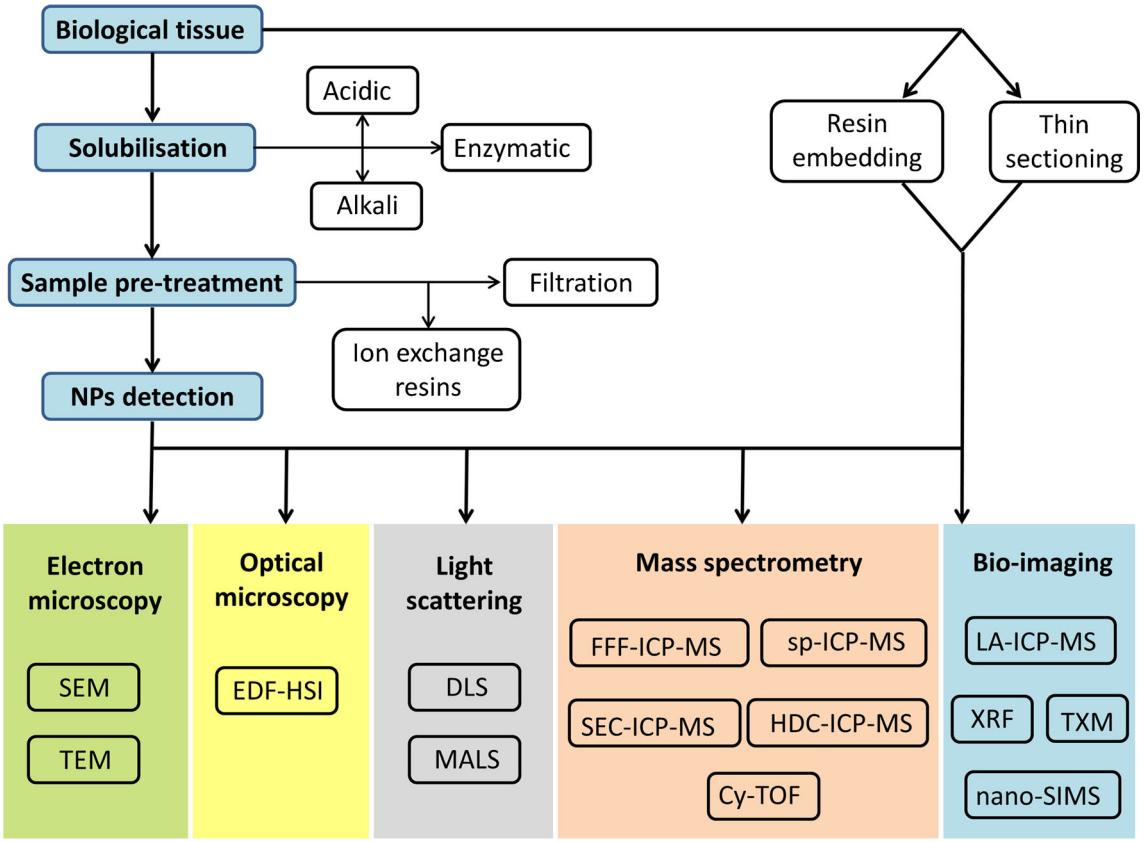

Fig. 1 Schematic illustration of individual NP analysis steps. SEM—scanning electron microscope; TEM—transmission electron microscope; EDF-HSI—enhanced darkfield hyperspectral imaging; DLS—dynamic light scattering; MALS—multi-angle light scattering; FFF-ICP-MS—field flow fractionation inductively coupled plasma mass spectrometry; sp-ICP-MS—single particle ICP-MS; SEC-ICP-MS—size exclusion chromatography ICP-MS; HDC-ICP-MS—hydrodynamic chromatography ICP-MS; Cy-TOF—mass cytometry; LA-ICP-MS—laser ablation ICP-MS; XRF—X-ray fluorescence; TMX—transmission X-ray microscopy; nano-SIMS—nano-secondary ion mass spectrometry.

Optical microscopy

The superior spatial resolution of electron microscopy overshadowed light scattering microscopy; however, this technique is being revitalised with the recent use of an enhanced darkfield hyperspectral imaging (EDF-HSI) [14–17]. The advantage of EDF-HSI over conventional optical spectroscopy is that under high-intensity darkfield conditions, the intensity of particle illumination is 150-fold higher resulting in a much brighter appearance of NPs and thus enables to record full visible and near-infrared spectra for each pixel within the image. Analysis using EDF-HSI is carried out under atmospheric pressure, and because it can handle wet samples with minimal preparation, it can be used for in situ time-dependent monitoring of NP behaviour [16]. Pena at al. conducted a comprehensive comparison study between EDF-HSI, Raman spectroscopy, energy dispersed X-ray spectroscopy and SEM in order to assess capabilities of EDF-HSI [18]. Porcine skin tissue was exposed to ceria and alumina NPs to serve as a toxicological model for cutaneous exposure and selected techniques were used for localisation and chemical identification of the detected NPs. The authors concluded that EDF-HSI is not only a suitable alternative to conventional methods but it outperforms other techniques in the speed of analysis and instrumentation cost.

Light scattering

Light scattering techniques such as multi-angle light scattering (MALS) and dynamic light scattering (DLS) are high-throughput techniques for analysis of NPs in aqueous media. Size parameters such as radius of gyration using MALS are determined by average intensities of the scattered incident light collected at several angles. On the other hand, DLS measures the Brownian motion of the NP via a time-dependent fluctuation in scattering intensity. This fluctuation is caused by constructive and destructive interferences and directly relates the movement to an equivalent hydrodynamic diameter [19]. However, the Brownian motion of the NP is affected by the viscosity of the media and the light scattering is dependent on the refractory index, which are very often difficult to determine. Additionally, DLS and MALS are not suitable for

analysis of samples with particles of heterogeneous size distribution due to an inherent discrimination of these techniques against small particles [20]. Therefore, hyphenation with size separation instruments such as field flow fractionation (FFF) or hydrodynamic chromatography (HDC) is very often used. Recently, Correia and Loeschner developed an analytical method for detection of nanoplastics in fish tissue using FFF coupled to a MALS detector [21]. While this method was successfully applied for detection of polystyrene NPs, the authors found interfering background light scattering too high for detection of polyethylene NPs. In another study, DLS detector coupled to a sedimentation FFF was used for detection of SiO_2 NPs in the lung tissue after enzymatic digestions [22]. The proposed method enables detection of 25 μg of 70-nm-size NPs per injected volume, a concentration relevant for the analysis of NPs in environmental samples.

Inductively coupled plasma mass spectrometry

High sensitivity, low detection limits, broad dynamic range and multi-isotope detection capabilities made ICP-MS an incredibly versatile instrument utilised in a very wide spectrum of scientific disciplines. In the context of NP analysis, ICP-MS has been used for nearly two decades [23] and the growing nanotechnology field had driven the improvement of the analytical performance of ICP-MS for NP characterisation at record speed. Among different ICP-MS available on the market, quadrupole (ICP-Q-MS), scanning sector field (SF-ICP-MS), static sector field with multi-collector detector (MC-ICP-MS) and time of flight (ICP-TOF-MS) are the most commonly used with each providing various advantages and disadvantages.

The most commonly used ICP-MS for NP analysis is ICP-Q-MS, which provides a very fast data acquisition time, a crucial parameter if you are to sample a particle event of less than about 0.5 ms in length [24]. To obtain detailed information about this short transient signal data acquisition system of at least 10^4–10^5 Hz is required and currently provided by several manufacturers. However, besides fast data acquisition time, sensitivity, defined as counts per second per unit concentration, is absolutely crucial for the detection of small NPs. The diameter of a spherical particle is a function of the cube root of the mass, i.e. the signal, and therefore, a small reduction in particle diameter causes a large decrease in the signal. Additionally, sensitivity also impacts on the precision caused by signal variation, and thus, more sensitive instruments provide higher precision in the analysis of small NPs. Applications of ICP-Q-MS were until recently limited to detection of one *m/z* at a time due to a settling time which is defined by the manufacturer and can be up to a few milliseconds long. Settling time is required for the quadrupole to stabilise for the measurement of the next *m/z*, and therefore, it was not viable to simultaneously collect data for multiple isotopes within a short dwell time required for NP detection. But interestingly, a recently published performance comparison between ICP-Q-MS and ICP-TOF-MS focusing on the multi-elemental analysis of NPs concluded that ICP-Q-MS with a settling time of 120 μs and shorter is capable of accurately detecting and sizing NPs with two elements [25].

Mass analyser of scanning SF-ICP-MS is constructed by a series of magnetic and electronic fields through which passing ions are doubly focused before reaching a detector. The double focusing feature of SF-ICP-MS results in superior resolution of mass discrimination, which so far cannot be matched by ICP-Q-MS. However, the trade-off for the superior resolution is the loss of sensitivity. And although SF-ICP-MS can acquire data at high acquisition frequency (10^4 Hz), analysis of selenium or arsenic NPs which requires a high resolution will result in a significantly higher particle size detection limit in comparison with ICP-Q-MS [26].

Following high demand for precise isotope ratio measurements, the manufacturer of SF-ICP-MS used the design of double focusing for high resolution but replaced the detector by multiple Faraday cups which are able to simultaneously collect several isotopes [27, 28]. While this instrumental setup could provide valuable information about possible changes in isotope fractionations in NPs, the signal acquisition frequency is not fast enough (10 Hz) for conventional NP analysis. The main restrictions for fast data acquisition are in the relatively slow time response of Faraday cups [29]. Furthermore, the current design of MC-ICP-MS does not allow acquisition of full mass spectra, but is restricted to a narrow *m/z* range.

Time of flight (TOF) mass analyser separates ions based on their velocities. Ions in an extraction region are accelerated by a short electric pulse to the field-free drift tube giving them same kinetic energy. Having the same kinetic energy means that ion velocities are defined by their *m/z*, and thus, ions of different *m/z* arrive at the detector at a different time. Although the detected ions originate from the same extracted portion of ions but because they are detected sequentially, the detection principle of ICP-TOF-MS is referred to as quasi-simultaneous [30]. Nevertheless, ICP-TOF-MS is capable of providing quantitative results of full mass spectra at a dwell time of 33 μs which makes it currently the only ICP-MS instrument which allows for multi-elemental analysis of a short transient signal generated by NPs. However, the detection of full mass spectra without compromising the resolution and maintaining a wide dynamic range (10^5–10^6) [31, 32] requires high-speed electronics, large data storage space and high computing power for the large amount of data generated, which are reflected in the high price of the instrument.

Fractionation and chromatography

Field flow fractionation technique is a flow-based fractionation, which takes place in a trapezoidal channel without a

stationary phase; thus, FFF does not classify as a chromatography technique. The trapezoidal channel is continuously filled with a carrier liquid and due to the geometry of the channel, the carrier liquid forms a parabolic flow profile, with the lowest velocity closest to the channel walls. The injected sample is first focused at the bottom of the channel, and subsequently, a perpendicular (cross) flow to the diffusion path is applied which aids the fractionation. Particles (or molecules) interacting with the cross flow will achieve different flow-profile velocities and smaller particles will elute first under normal mode. The perpendicular field which provides the necessary interaction with particles and thus their fractionation can vary and several sub-categories of FFF are available; asymmetric flow FFF (AF4), sedimentation FFF (sdFFF), thermal (Th-FFF), magnetic (Mg-FFF) and electrical (El-FFF) [33, 34]. FFF can be coupled to various detectors but its hyphenation with ICP-MS became dominant in the analysis of engineered NPs present in environmental and biological matrices. This instrumental setup was successfully used for detection of Ag NPs in the gastrointestinal tract and gill tissue of *Pimephales promelas* [35] and chicken meat [36, 37] but also SiO_2 NPs in food products [38] and bovine serum [39].

Another technique which allows for separation of different-size NPs and can be coupled to either light scattering detectors or ICP-MS is size exclusion (SEC) and hydrodynamic chromatography (HDC). Both methods separate particles based on their hydrodynamic volume; however, SEC columns are packed with porous particles, whereas the particles in HDC columns are non-porous or with very small pores. Packing materials of these columns define the mechanism of particle separation. In SEC columns, separation takes place through a reverse-sieving mechanism based on the relative size of analyte NPs and the pores of the packing materials. Large NPs elute first as they enter fewer pores or sampler smaller pore volume [40]. On the other hand, separation in the HDC column is due to parabolic flow velocity in the open tube channel, which leads to small particles being closer to the walls where the flow is stagnant and larger particles being near the center where the flow is faster [41]. Thus, in both techniques, large particles have shorter retention time. While both of the techniques are capable of successfully separating NPs of varying size, they are not very popular for several reasons. Similar to FFF, using SEC or HDC for chromatographic separation of NPs requires long analysis time per sample, typically around 30 min. Additionally, due to a low injection sample volume, generally 20 μL, the particles are heavily diluted during the elution and thus environmentally relevant concentrations may fall below the detection limits. Also, adsorption of NPs on the column packing material has been reported, which results in a lower analyte recovery [42].

X-ray tomography

Other, less commonly used techniques for imaging of NPs are X-ray-based techniques such as X-ray fluorescence (XRF) and transmission X-ray microscopy (TXM). While the former can produce two-dimensional images representative of the elemental distribution of monitored analyte, the latter technique is capable of generating images of three dimensions. Synchrotron-generated beam used for XRF can typically provide a spatial resolution between 1 and 10 μm, whereas some beamline facilities focusing on sub-micrometer analysis are able to provide an enhanced spatial resolution < 100 nm [43]. Despite the lack of necessary spatial resolution, XRF provided essential information in the investigation of CeO_2 NP deposition in rat lung tissue [44] and earthworms [45], as well as uptake of TiO_2 and multiwalled carbon nanotubes by zebra fish [46] and skin penetration of Au nanorods [47]. On the other hand, modifications of micro-zone plates, which are used in the projection of a full-field image to an X-ray-sensitive device, improved the spatial resolution of TXM to < 20 nm. Such modification allowed visualisation of Au NPs biosynthesised by *Saccharomyces cerevisiae* [48, 49]. However, imaging techniques are not able to distinguish between the physical states of the analyte, and thus, high signal intensity generated by the analyte does not guarantee that the analyte is present in particulate form. Nonetheless, tomography plays an important role in the mapping of NP distribution within the living organisms as well as in the understanding of biological processes leading to their formation [43, 50].

Increasing need for (certified) reference materials

According to the ISO definition, a reference material (RM) is "material, sufficiently homogeneous and stable with respect to one or more specified properties, which has been established to be fit for its intended use in a measurement process" [51]. On the other hand, a certified reference material (CRM) is a special subset of reference materials defined as "reference material characterized by a metrologically valid procedure for one or more specified properties, accompanied by a certificate that provides the value of the specified property, its associated uncertainty, and a statement of metrological traceability" [51]. These materials play a pivotal role in the development and validation of analytical methods in terms of method trueness, precision and proficiency. However, the current analytical methods suffer from the lack of suitable RMs and CRMs. For instance, the single-particle ICP-MS method requires the calculation of transport efficiency (nebulisation efficiency) which can be determined only by using a well-defined material in terms of its particle number concentration and particle size. Generally, Au NP SRM 8013 is being cited in the literature, regardless that the actual analyte NPs do not contain Au or are of a different size than SRM 8013. This

might have potential implications on the calculated particle number concentration in the actual samples as the transport efficiency may differ with the size of the NPs and also the plasma ionisation efficiency varies across the periodic table. Additionally, currently available RMs and CRMs are dominated by mono-elemental NPs (Table 1); however, engineered NPs released to the environment as well as naturally formed NPs resemble more closely to nanocomposites. The development of NP RMs and CRMs is not an easy task [52]; however, with the increasing demands from the regulatory agencies for the monitoring of NPs, we can expect more products in the market in the near future.

Sample preparation for analysis of NPs in biological matrices

In order to investigate physical alterations of NPs induced by its host environment, reliable methods that ensure isolation of NPs from the tissue without unintentional modifications are required. Tissue degradation using acidic or basic condition may lead to particle dissolution or aggregation which will provide false information about the physical state of the particles. Acid solubilisation for the liberation of NPs from the tissue matrix is generally not recommended as it significantly alters the surface of NPs. Arslan et al. showed that ultrasonication of CdSe NPs in 0.5% HCl promotes aggregation of NPs most probably as a result of the dissolution of thiol capping on the surface of the particles [53]. Furthermore, increased concentration of ionic Cd was found in the solution indicating that some of the CdSe NPs underwent dissolution. On the other hand, the impact of alkali and enzymatic solubilisation on the NPs seems to be more complex and the published results suggest that more factors may affect the efficiency of these methods. Tetramethylammonium hydroxide (TMAH) is most commonly used in alkali solubilisation [54–57]; however, KOH and NaOH were also used within the medical community [58, 59]. While the reported studies agree that TMAH is effective in tissue solubilisation, its impact on NP stability is disputed. Ultrasonication of CdSe NPs suspended in the solution of 10% (*v*/*v*) TMAH had no effect on the NPs; however, heating of the solution promoted aggregation of the NPs, but no release of ionic Cd was observed [53]. Similarly, aggregation of Ag NPs was observed when biological tissue was solubilised in 20% TMAH, and furthermore, the formation of Ag NPs was found when a control tissue digest was spiked with ionic Ag [60]. On the contrary, Gray et al. reported no observable alteration in the Ag NPs extracted from biological tissue testing several concentrations of TMAH although the data suggest a slight shift towards a larger particle size [61]. In a similar way, enzymatic solubilisation is widely implemented for the liberation of NPs from various biological matrices [12, 36, 54, 60, 62–65]. Proteases are the most commonly used enzymes for animal tissues generally in combination with sodium dodecyl sulfate (SDS) acting as surfactant and sodium azide to prevent bacterial growth. Campbell at al. reported only partial digestion of muscle tissue; however, the digestion was performed at 60 °C, and thus, the incomplete digestion could be a result of protein denaturation [58]. Similarly, low recoveries of SiO_2 NPs separated from lung tissues were reported when a mixture of collagenase and hyaluronidase was used, followed by

Table 1 Overview of available NPs CRMs

NP type	Element	Name	Specification (nm)	Producer
Metal/loid	Au	SRM 8011	10	NIST
		SRM 8012	30	
		SRM 8013	60	
	Ag	SRM 8017	75	
	Si	SRM 8027	2	
Metal oxides	SiO_2	ERM-FD100	20	EC-JRC
		ERM-FD101b	80	
		ERM-FD102	bimodal: 18–85	
		ERM-FD304	40	
Organic	Polystyrene spheres	SRM 1964	60	NIST
		SRM 1963a	100	
		SRM 1691	300	
	SWCNT	SWCNT-1	1.5	NRC
	Cellulose nanocrystals	CNCS-1	84 × 5.6	
		CNCD-1	87 × 35	
		CNC-1	133 × 4.1	

SWCNT single-wall carbon nanotube, *NIST* National Institute of Standards and Technology, *EC-JRC* European Commission Joint Research Center, *NRC* National Research Council of Canada

proteinase K, which was incubated at 65 °C [22]. On the contrary, studies that perform tissue solubilisation with proteinase K at a temperature between 34 and 37 °C report complete breakdown of the tissue matrix. The published results also suggest that NPs suffer fewer or none of the physical alternation observed under TMAH conditions when proteinase K is used. No aggregation or dissolution of Ag NPs was observed, and similarly, the formation of NPs was not detected when control tissue was spiked with ionic Ag [60]. An overview of selected digestion methods can be found in Table 2.

Furthermore, since the toxicity of some NPs, e.g. Ag NPs, is related to the release of Ag^+ from Ag NPs and analytical methods such as the single-particle ICP-MS are greatly affected by the presence of the dissolved analyte of interest, the extraction and/or sample preparation method should be able to minimise or eliminate the presence of these ions. The two most common scenarios are either to immobilise the ionic species or capture the particles and wash out the ions. The former one can be done by coupling ion exchange resins prior to ICP-MS as it was demonstrated by utilisation of Chelex 100 resin for binding Ag ions in the solution containing both dissolved and particulate Ag [67]. To perform the latter, HgSe nanoparticles were captured using low molecular cutoff filters, which allowed the dissolved species to pass through [62]. Captured particles were further washed several times with ultra-pure water and then re-suspended in aqueous media. Both methods achieved a significant reduction of the background concentration of studied analytes and thus improved the limit of detection of sp-ICP-MS.

New insights into engineered NP behaviour in biological tissue

The past decade of engineered NP analysis–driven improvements in the capabilities of the analytical instrumentation provided a solid platform for investigations into NP behaviour in living organisms. Heringa et al. investigated the presence of TiO_2 NPs in 15 post-mortem human livers and spleens from individuals whose occupational exposure to TiO_2 was excluded [68]. By using sp-ICP-MS, the size distribution of Ti NPs was found to be between 85–550 and 85–720 nm in the liver and spleen, respectively. In order to corroborate the aggregation state and chemical composition, the group used SEM-EDX and found that the particles consist of Ti and O and underwent agglomeration and/or aggregation of smaller primary particles (Fig. 2). Strikingly, the size distribution of TiO_2 NPs found in the tissues fell within that of TiO_2 food particles (30–600 nm) [69] which indicates that the particle found were of dietary origin. Moreover, the concentration levels of TiO_2 in the liver were above the level at which an adverse effect may occur in humans.

Another study showed that while CeO_2 and TiO_2 NPs administered through oral gavage to mice were completely excreted from the body, pulmonary-administered NPs were found in the liver [70]. The visualisation of NPs in the affected tissues was done by SEM equipped with STEM detection and EDF-HSI. Quantitation of translocated NPs by sp-ICP-MS showed that up to 2.87% of CeO_2 and 1.24% of TiO_2 NPs were deposited in the liver 180 days following the inhalation of NPs. Size distribution of CeO_2 showed that the NPs underwent partial dissolution as they were found in a smaller size (25 nm) in comparison with the original size of 35 nm at the time of exposure. In vivo fragmentation of CeO_2 was previously reported, where cube-shaped CeO_2 was found rounded along the edges after 90 days of residing in the liver tissue [71]. Interestingly, large amounts of ultrafine crystallites (1–3 nm) were found in close proximity of the rounded CeO_2 NPs which were labelled as CeO_2 clouds.

The antibacterial properties of Ag NPs made them extremely popular in wound dressings where they are in direct contact with an open wound and thus can be taken up by the systemic circulation and translocated into other organs. NP translocation and their ability to cross physiological barriers can be particularly dangerous for the developing foetus without effective defence mechanism. Several studies showed that SiO_2, TiO_2 NPs and single-wall carbon nanotubes can cross the placental barrier in rodents and cause foetal complications [72–75]. Recently published study using ex vivo human placenta perfusion model found Ag NPs on the foetal circulation side after exposure to Ag NPs and ionic Ag [17]. Because Ag NPs are water soluble, it could not be determined whether the NPs found on the foetal circulation side are a result of NP translocation across the placental barrier or their dissolution on the maternal circulation side, diffusion of ionic Ag across the barrier and subsequent formation of NPs on the foetal circulatory side. Single-particle ICP-MS analysis of Ag NPs on the foetal circulatory side after exposure to Ag NPs and ionic Ag did not reveal any significant difference between formed NPs, and thus, it was not possible to identify which deposition path took place.

Understanding the biological response to NP exposure and their translocation within the organism is a very complex task, which requires the knowledge of NP localisation on cellular and subcellular levels. Techniques such as laser ablation coupled to ICP-MS (LA-ICP-MS) or synchrotron XRF tomography can be useful; however, they generally lack the spatial resolution at the nanometre scale. Laser ablation coupled to ICP-MS was recently used to investigate Au and Ag NP uptake by unicellular organisms, and using a laser spot size of 4 μm, the authors were able to locate accumulation of NPs in a perinuclear region [76]. However, as this analytical technique is blind to the physical state of the analyte, without the prior knowledge of the physical characteristics, it

Table 2 Summary of sample preparation protocols for analysis of NPs in biological tissue

Tissue type	Analyte	Reagent	Protocol	Instrument	Reference
Chicken meat	Ag NPs	Proteinase K	0.2 g of tissue was vortexed (1 min) in buffer (10 mM Tris buffer, 1% Triton X-100, 1 mM $Ca(OAc)_2$, pH 9.5) and sonicated for 5 min on ice. 25 μL of proteinase K was added, and the sample was incubated for 3 h at 35 °C.	sp-ICP-MS	[65]
Human tissue	Ag NPs	TMAH	0.2 g of tissue homogenate was mixed with 0.3 mL of UPW and 2 mL of TMAH (25% *v*/*v*). Sample was sonicated for 1 h at RT and subsequently mixed on a wheel rotator at RT for 23 h.	sp-ICP-MS	[60]
		Proteinase K	3 g/L of proteinase K and 0.5% SDS were diluted in enzyme buffer (50 mM NH_4HCO_3 and 200 mg/L NaN_3 at pH 7.4). 0.2 g of homogenate was mixed with 2 mL of the enzyme solution and left in the water bath for 1 h at 37 °C.	sp-ICP-MS	
Rat liver	Au NPs	TMAH	Bovine serum albumin was added to 2 mL of liver homogenate at approximately 10-fold excess by mass relative to the Au content. TMAH was added in a final concentration of 5% (*v*/*v*). The samples were sonicated (1 h) and rotated mechanically at RT overnight.	AF4-ICP-MS	[66]
Rat liver and kidney	CdSe	TMAH	Sample (ca. 0.25 g wet weight) was digested with 4 mL of 25% (*m*/*v*) TMAH at 70 °C for 2 h.	sp-ICP-MS	[53]
Whale liver and brain	HgSe NPs	Proteinase K	Freeze-dried tissue (~ 20 mg) was defatted by sonication in MeOH:DCM (1:2) for 5 min, and then, the enzyme solution (1 mg/mL of proteinase K in 50 mM NH_4HCO_3 buffer pH 7.4, with 5 mg/mL of SDS) was added. The mixture was incubated at 37 °C overnight.	sp-ICP-MS	[62]
Earthworms	Ag NPs	Collagenase, hyaluronidase and proteinase K	Firstly, sample was incubated overnight (18 h) at 37 °C in 500 μL of collagenase (10 mg/mL) and 1.5 mL of hyaluronidase (90 mg/mL) with shaking. Afterwards, 500 μL of proteinase K (1 mg/mL) was added and the sample was incubated for 2 h at 65 °C.	sp-ICP-MS, SEM	[12]
Chicken meat	Ag NPs	Proteinase K	Sample was vortexed (1 min) in 5 mL of the proteinase K solution (3 mg/mL proteinase K, 50 mM NH_4HCO_3 buffer at pH 7.4, 5 mg/mL SDS and 0.2 mg/mL NaN_3). The mixture was incubated at 37 °C in a water bath while stirred for 40 min.	AF4-ICP-MS	[36, 37, 54]
Mammalian liver and lung	SiO_2	Collagenase, hyaluronidase and protease	Collagenase (150 U/mL) and hyaluronidase (100 U/mL) were added to the homogenised tissue and incubated overnight at 37 °C with shaking. An ultrasonic processor was used for tissue processing, followed by incubation with 200 μg/mL proteinase K in 0.5% SDS for 2 h at 65 °C.	sdFFF-DLS, TEM, Fluorescence microscopy	[22]
Beef, *Daphnia magna*, *Lumbriculus variegatus*	Ag NPs, Au NPs	TMAH	0.5 g of tissue was solubilised in 10 mL of TMAH (20% *v*/*v*) for 12 to 24 h with the first hour for sonication.	sp-ICP-MS	[61]
Yeast	Se NPs	Enzymatic mix	(1) 0.2 g of yeast were sonicated with 5 mL of UPW for 5 min and centrifuged. (2) Pellet was re-suspended	sp-ICP-MS, SEC-ICP-MS, TEM	[13]

Table 2 (continued)

Tissue type	Analyte	Reagent	Protocol	Instrument	Reference
			in of 4% Driselase in 30 mM Tris buffer (pH 7.5) and incubated for 17 h at 25 °C, followed by centrifugation. (3) Pellet was re-suspended in 5 mL of protease (4 mg/L) in 30 mM Tris buffer (pH 7.5), incubated for 17 h at 37 °C and centrifuged. (4) Pellet was re-suspended in 5 mL of 4% SDS and sonicated for 1 h, followed by centrifugation.		
Fish tissue	Nanoplastics	Proteinase K	0.1 g of fish slurry was mixed with 51 mL of the proteinase K solution (3 mg/mL proteinase K, 47 mM NH_4HCO_3 buffer at pH 7.7, 5 mg/mL SDS and 0.2 mg/mL NaN_3). The mixture was incubated at 37 °C in a water bath for 17 h while stirred.	AF4-MALS, AF4-LS, SEM	[21]
Rat faeces	Ag NPs	TMAH	100 mg ground sample was mixed with 2 mL of TMAH (25% *w/w*) and 400 mL of cysteine (0.5% *w/w*) in a tumbler for 24 h at 28 rpm.	AF4-UV/vis, TEM, LA-ICP-MS	[55]

$Ca(OAc)_2$ calcium acetate, *TMAH* tetramethylammonium hydroxide, *UPW* ultra-pure water, *RT* room temperature, *NH_4HCO_3* ammonium bicarbonate, *NaN_3* sodium azide, *SDS* sodium dodecyl sulfate, *DCM* dichloromethane, *sp-ICP-MS* single-particle inductively coupled plasma mass spectrometry, *TEM* transmission electron microscope, *AF4* asymmetric flow field flow fractionation, *SEM* scanning electron microscope; *sdFFF* sedimentation field flow fractionation, *DLS* dynamic light scattering, *SEC* size exclusion chromatography, *MALS* multi-angle light scattering, *LS* light scattering, *LA* laser ablation

would not be able to identify whether the signal intensity is generated by NPs or accumulation of dissolved ions. On the other hand, imaging techniques such as EDF-HSI has become increasingly popular as it can provide the necessary spatial resolution, down to the nanometre scale together with the chemical analysis of NPs. Intracellular uptake and associated toxicity of Ag NPs was investigated in *Caenorhabditis elegans*, upon their exposure to three types of Ag NPs [15]. Exposure of *C. elegans* to 3-nm in-house-synthesised Ag NPs led to the internal retention of developed eggs, which is a common response of *C. elegans* to stress conditions. Furthermore, using EDF-HSI, the authors were able to localise Ag NPs within the fertilised egg (Fig. 3) and thus provided evidence that the low-nanometer-size Ag NP can transverse the cell membranes and can be passed from one generation to the other. More interestingly, Mortimer et al. tested the capabilities of EDF-HSI to distinguish between two different NPs taken up by the same cells [14]. EDF-HSI analysis of protozoa cells exposed to Ag NPs and quantum dots (QDs) showed that the spectral signatures from NPs and QDs were clearly distinguishable from each other although the higher agglomeration of QDs made the analysis challenging.

Analysis of naturally formed nanoparticles

Naturally formed NPs are generally under-researched although there is substantial evidence that detoxification of several metals takes place via formation and deposition of NPs. For instance, the first reports of observed formation of dense particulate matter containing Hg and Se in the tissues of marine mammals were published over four decades ago [77]; however, very little was revealed about their physical and chemical composition. Comprehensive analysis of naturally formed NPs is very challenging due to a large number of unknowns right from the start. Naturally formed NPs will very rarely be mono-elemental, considering the biological processes involved in detoxification; hence, their chemical composition will most probably resemble nanocomposites. Their chemical stability towards the extraction protocols is unknown and size distribution may vary significantly with no one size being dominant. Such a non-homogeneous distribution eliminates the use of size separation techniques such as FFF, HDC or SEC due to a lack of resolution. The size determination using sp-ICP-MS might be inaccurate as the mathematical conversion of signal intensity to particle size requires the knowledge of the particle's density, which could only be an estimate without knowing the chemical composition of the NPs. Nonetheless, the information provided by studies of naturally formed NPs are

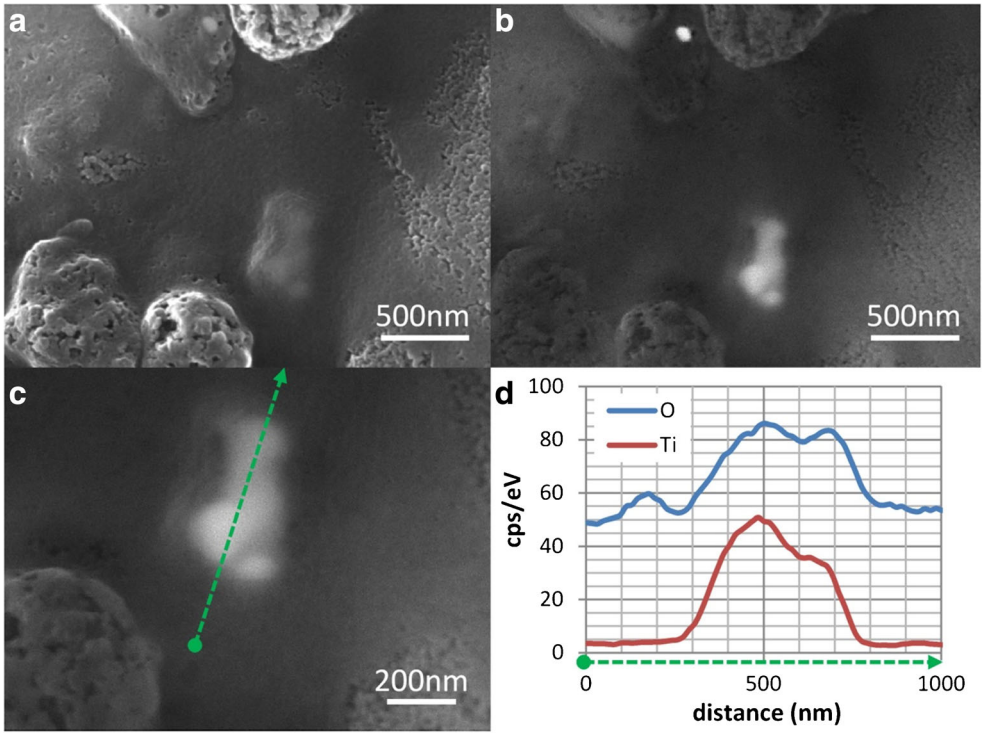

Fig. 2 SEM characterisation of detected TiO_2 particles in a dried liver sample. **a** The secondary electron microscope image shows a TiO_2 agglomerate below the surface of the liver tissue (arrow). **b** The backscattered electron image reveals the spherically shaped primary particles within the agglomerate (arrow), with diameters between 75 and 150 nm. **c** The path of the EDX line scan across the aggregate in the same image at higher magnification. **d** The presence of TiO_2 based on the corresponding increase of response for Ti (red line) and oxygen (blue line) at the position of the particle. This forms a clear indication that the detected particle is indeed TiO_2. Figure originally published in Heringa et al. [68]

crucial for the understanding of metabolic processes which take place under long-term exposure to environmental pollutants.

Gajdosechova et al. conducted a comprehensive investigation of Hg- and Se-containing NPs found in the liver and brain tissue of stranded long-finned pilot whales [62]. To identify the presence of NPs, LA-ICP-MS and synchrotron μXRF were used to visualise the particles (Fig. 4). As both techniques have multi-elemental capabilities, they were able to identify major elements, Hg and Se present in the particles by overlaying the intensity distribution maps constructed for each element. Furthermore, synchrotron μXRF was used for calculation of the molar ratio between Hg and Se within the mapped area. The presented correlation plot revealed differences in the molar ratios in the small NPs and large aggregates and thus indicating that not only the chemical composition of naturally formed NPs originated from presumably the same chemical reactions may significantly differ but also the formed NPs behave as reactive species and undergo physical and chemical alterations within the host organism.

For the size distribution of NPs, enzymatically solubilised tissue solutions were analysed using sp-ICP-MS acquiring *m/z* 202 and 78, for Hg and Se respectively. As the instrument used was quadrupole ICP-MS, this analysis could not be performed simultaneously but was carried out sequentially, and thus, the size distribution based on Hg and Se is reported [62]. The study found that the NPs undergo aggregation and/or agglomeration during the lifespan of the animal as well as the number of PNs within the brain and liver increases with the age of the animals.

Outlook

Nanoparticle analysis is incredibly dynamic field with very fast-evolving analytical techniques applicable in numerous disciplines. And although the development of analytical techniques for detection and quantitation of NPs in natural samples has been predominantly driven by the avant-garde of environmental analytical chemists, interdisciplinary dialogues are being established to develop new analytical techniques with a focus on better understanding of NP interactions with living organisms.

Analysis of NPs is dominated by sp-ICP-MS, also supported by the manufacturers who are improving the detection capabilities of mainly ICP-Q-MS with shorter dwell and settling times. These improvements provide a wider choice of the ICP-MS instrument suitable for NP analysis as well as overcome the limitation of single *m/z* monitoring [25], although still short of full mass range detection provided by ICP-TOF-MS. An increasing number of analytical chemists got involved in fine-tuning of the instrument performance and provided practical solutions for the observed limitations. For sp-ICP-MS to become a standard technique for regulation purposes, it has to be accurate, and presently, the accuracy of particle sizing and concentration determinations is decreased

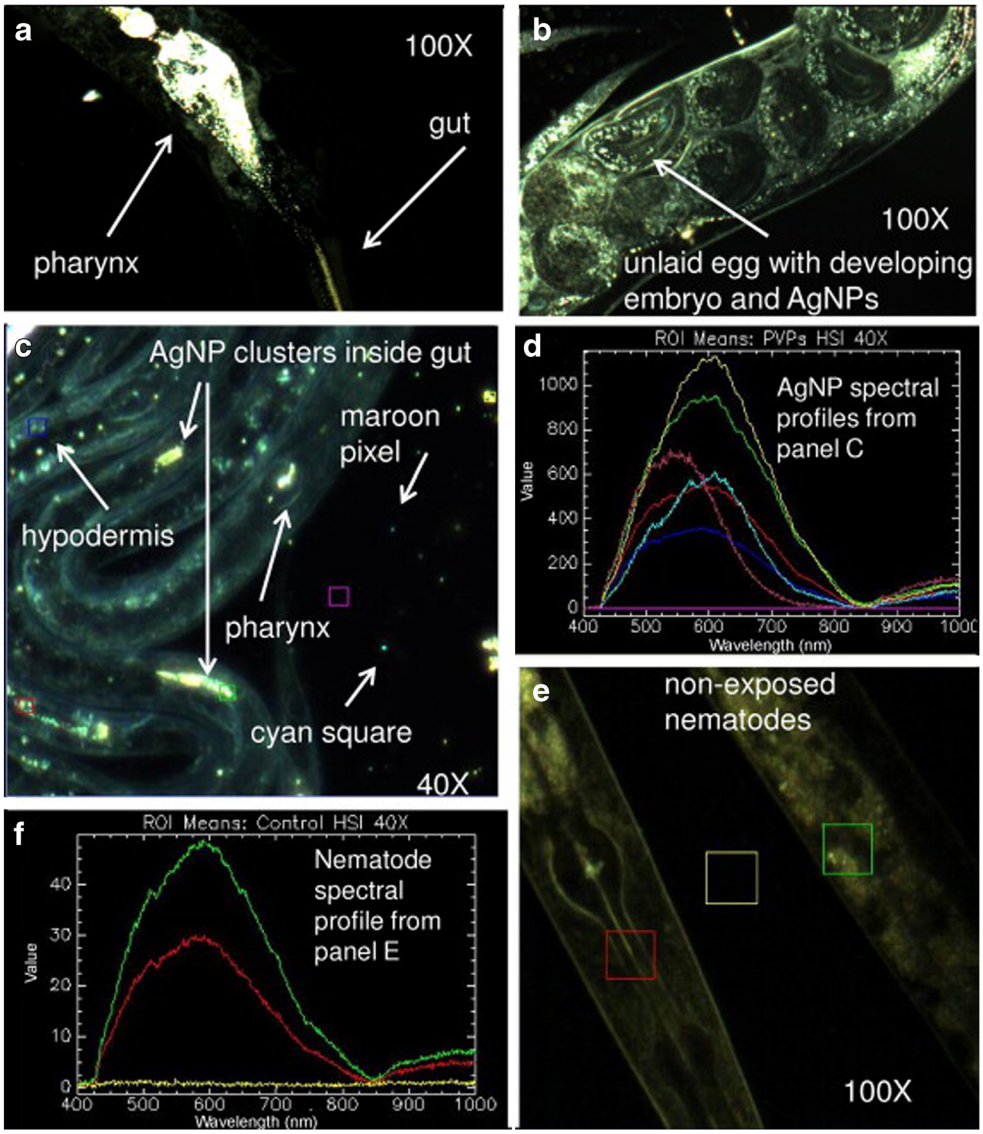

Fig. 3 AgNPs are ingested and internalised into the cells of *C. elegans*. **a** CIT_{10} AgNPs are taken up along with food by *C. elegans*. **b** Some CIT_{10} AgNPs are also taken up into the cells of the nematodes and are transferred to the offspring. AgNP identity was confirmed by hyperspectral analysis. **c** Hyperspectral image (HSI) showing the presence of PVP AgNPs inside and outside *C. elegans* after exposure; coloured rectangles correspond to the pixel areas (regions of interest (ROI)) in HSI where spectral profiles are collected. **d** The spectral profiles of AgNPs and hypodermis region of *C. elegans*: green, red, and dark blue represent internal AgNPs clusters; yellow, cyan and maroon external AgNP clusters; and magenta background. **e** and **f** Very little signal is detected in non-exposed nematodes; note that *y*-axis values are much lower in (**f**) than (**d**); a higher contrast was used in (**e**) than (**c**) for visualisation. Images taken using CytoViva hyperspectral imaging technology with darkfield microscopy at × 100 (panels **a**, **b** and **e**) or ×40 (panel **c**) total magnification. The colour of the spectral profile corresponds to the colour of the rectangle in the image and each profile represents the average of all the pixels present in each square. Reproduced from Meyer et al. [15] with permission from Copyright Clearance Center's RightsLink® service

by a high uncertainty in the transport efficiency [78]. Tuoriniemi et al. suggested a method for the calculation of a correction factor which reduces the uncertainty in transport efficiency; however, further developments are still needed for this method to become fully reliable [79]. Another improvement in terms of sample uptake and introduction is the development of the micro-droplet generator (MDG) which is being used in place of the pneumatic nebuliser. Micro-droplet generator introduces into the plasma very low sample volume, which in turn eliminates matrix effect and facilitates analysis of high salt content solutions without the necessary de-salting steps. More importantly, comparative studies looking at transport efficiency between MDG and pneumatic nebuliser showed that an average 7% transport efficiency provided by pneumatic nebuliser can be increased by MDG to 100% [80]. These improvements only suggest that sp-ICP-MS will continue to be the primary method for NP analysis in the near future.

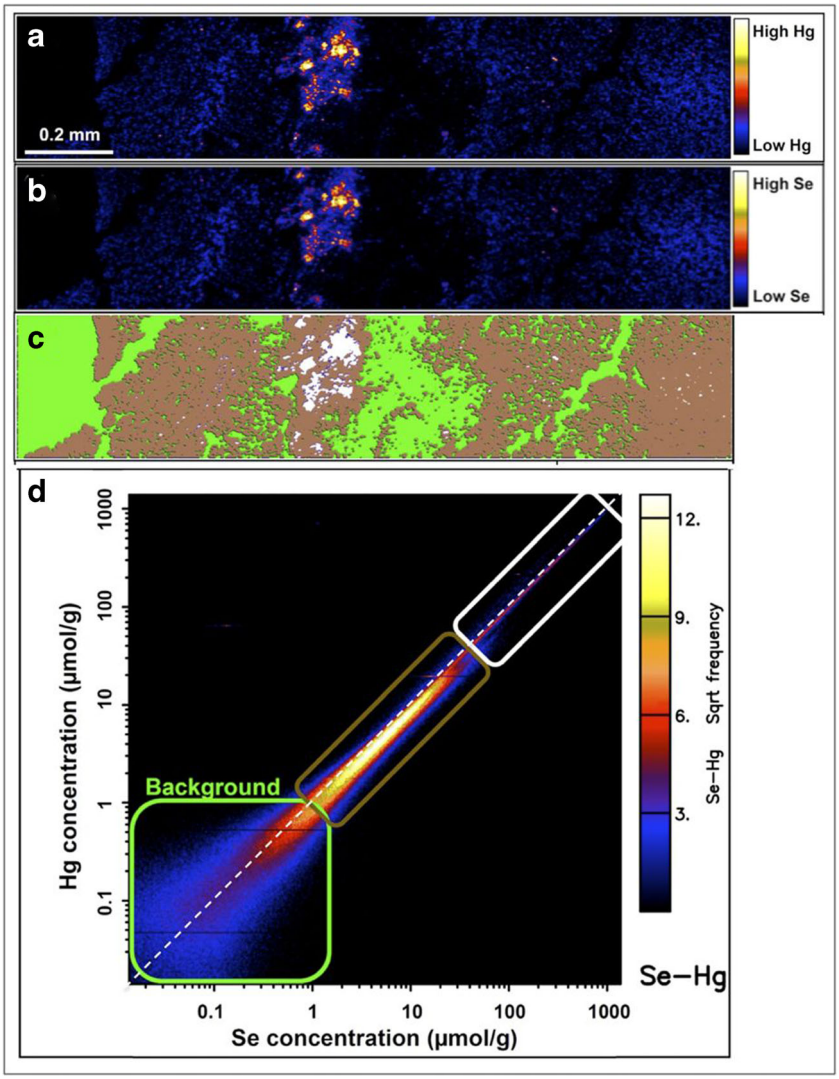

Fig. 4 2D map of Hg (**a**) and Se (**b**) distribution in the liver of an adult whale generated by synchrotron μXRF from a 30-μm thin section. Hg clusters are visible in the areas of high Hg intensity (yellow/white), which corresponds with Se distribution. Diffused Hg and Se are illustrated in blue. In **c**, the elemental map of Hg from (**a**) is overlaid with the three pixel populations identified using the 'elemental association' module in GeoPIXE, with each pixel population corresponding to the coloured boxes in the element correlation plot in (**d**). Se:Hg molar ratio of 1 is highlighted in (**d**) by a diagonal white dashed line. The white rectangle is corresponding to white pixels in the map (**c**), the aggregates in the map (**a**) with Se:Hg molar ratio of 1. Areas of low Hg concentration (blue in map (**a**), represented in brown in map (**c**) show a skewed elemental association towards higher Se in the plot (**d**) with Se:Hg molar ratio > 1. Figure originally published in Gajdosechova et al. [62]

Translocation of NPs within the living organism as it was observed in ex vivo human placenta studies of Ag NPs [17] brought up a new question about the true origin of NPs. Similarly, in the case of naturally formed NPs, it is not clear whether NPs are formed within one organ and subsequently transported through systemic circulation or whether they are formed locally. These questions could be answered by comparing the isotope ratios and identifying mass-dependent fractionation (MDF) of a given element using MC-ICP-MS. Although not observed for all, some elements such as Ag or Hg undergo MDF which is mainly a result of biological processes and reaction kinetics, including species transformation during detoxification, metabolism and biological transport [81]. Mass-dependent fractionation causes enrichment of the organ of origin in the heavier isotopes; thus, the destination organ is enriched in the lighter isotopes which helps to clarify whether NPs were transported or formed in the given organ. So far, applications of MC-ICP-MS for NP analysis were only scarcely explored, partly due to the low sensitivity of these instruments, but also owing to their cost, they are not widely available. Nonetheless, they can contribute pertinent information about the NPs' origins, and thus, it can be expected that new studies will explore these possibilities.

Nano-SIMS (secondary ion mass spectrometry) is a mass spectrometry-based technique which provides high sensitivity and high resolving power (> > 10,000) as well as high lateral resolution down to 50 nm and so far is mainly used in biological sciences [82]. Nano-SIMS enables multi-elemental as well as multi-isotopic analysis and imaging at the subcellular level and repeated sample irradiation offers the possibility of in-depth profiling, resulting in the construction of 3D images. It has been applied for investigations of Ag [83–85] and TiO_2 [86, 87] NPs' effects in living organisms in combination with other analytical techniques. One of the great advantages of nano-SIMS is its ability to detect the so-called "forbidden *m/z*" for ICP-MS such as C, H and N, and thus, it widens the range of NPs from mainly metallic which are the current focus of NPs

analysis to NPs such as black carbon, one of the most abundant NPs in the environment.

Another emerging technique that is based on the principle of flow cytometry but coupled to ICP-TOF-MS detector is mass cytometry or Cy-TOF. This technique is generally used for analysis of NPs within cells as it is equipped with specialised introduction system better suited for analysis of single cells. The cells or particles are introduced from a liquid suspension by the syringe pump and aspirated by a nebuliser, which is connected to a heated spray chamber. High flow (ca 5 L/min) of argon gas supplied to the spray chamber is heated which facilitates evaporation of aerosol droplets encapsulating cells or NPs. Dry cells or particles are then delivered to the plasma, where they generate an ion cloud and are analysed in a similar fashion to sp-ICP-MS [32]. Cy-TOF has been used for tracking the cellular uptake and bio-distribution of Au NPs [88] as well as intra- and extracellular Ag concentration in human T lymphocytes exposed to Ag NPs [89]. Cy-TOF has very high theoretical cell or NP analysis throughput, up to 3000 cells or NPs per second, which is physically limited by the need for separation of individual ion clouds formed in the plasma. However, such a fast data acquisition with multi-isotopic information produces a data set of high complexity, which requires bioinformatics for multi-parametric cytometry data sets. Additionally, if Cy-TOF is used for the analysis of single cells and their possible uptake of NPs, it is not able to identify potential dissolution or transformation of NPs in the cells, and thus, it should be used in combination with other techniques to get a definite confirmation that recorded intensities are from NPs and not a high concentration of dissolved analytes. But, as NP cytotoxicity is one of the main concerns in regard to environmental release of NPs and their interaction with living organisms, this technique provides some advantages over sp-ICP-MS.

To conclude, there is no one technique which can provide sufficient information about NP behaviour in the biological and environmental matrices, and thus, one can expect that the field of NP analysis will bring together scientists from a broad range of scientific disciplines with expertise in diverse analytical techniques. As it can be seen from the current analytical trends, a methodological cross-fertilisation is possible and we believe that it is the only way to answer some of the most challenging questions in NP analysis.

Compliance with ethical standards

Conflict of interest The authors declare that they have no conflict of interest.

Publisher's note Springer Nature remains neutral with regard to jurisdictional claims in published maps and institutional affiliations.

References

1. Hochella MF. Nanoscience and technology: the next revolution in the Earth sciences. Earth Planet Sci Lett. 2002;203(2):593–605. https://doi.org/10.1016/s0012-821x(02)00818-x.
2. Wang H, Pumera M. Fabrication of micro/nanoscale motors. Chem Rev. 2015;115(16):8704–35.
3. Karshalev E, Esteban-Fernández de Ávila B, Wang J. Micromotors for "Chemistry-on-the-Fly". J Am Chem Soc. 2018;140(11):3810–20.
4. Banfield JF, Zhang H. Nanoparticles in the environment. Rev Mineral Geochem. 2001;44(1):1–58. https://doi.org/10.2138/rmg.2001.44.01.
5. Naasz S, Altenburger R, Kühnel D. Environmental mixtures of nanomaterials and chemicals: the Trojan-horse phenomenon and its relevance for ecotoxicity. Sci Total Environ. 2018;635:1170–81. https://doi.org/10.1016/j.scitotenv.2018.04.180.
6. Communication from the Commission to the European Parliament, the Council and the European Economic and Social Committee on the Second Regulatory Review on Nanomaterials. 2012. https://ec.europa.eu/health//sites/health/files/nanotechnology/docs/swd_2012_288_en.pdf
7. Re-evaluation of titanium dioxide (E 171) as a food additive. EFSA J. 2016;14(9):e04545. https://doi.org/10.2903/j.efsa.2016.4545.
8. Gordon SC, Butala JH, Carter JM, Elder A, Gordon T, Gray G, et al. Workshop report: strategies for setting occupational exposure limits for engineered nanomaterials. Regul Toxicol Pharmacol. 2014;68(3):305–11.
9. Amenta V, Aschberger K, Arena M, Bouwmeester H, Moniz FB, Brandhoff P, et al. Regulatory aspects of nanotechnology in the agri/feed/food sector in EU and non-EU countries. Regul Toxicol Pharmacol. 2015;73(1):463–76.
10. Lapresta-Fernández A, Salinas-Castillo A, Anderson dela Llana S, Costa-Fernández JM, Domínguez-Meister S, Cecchini R, et al. A general perspective of the characterization and quantification of nanoparticles: imaging, spectroscopic, and separation techniques. Crit Rev Solid State. 2014;39(6):423–58. https://doi.org/10.1080/10408436.2014.899890.
11. Sadik OA, Du N, Kariuki V, Okello V, Bushlyar V. Current and emerging technologies for the characterization of nanomaterials. ACS Sustain Chem Eng. 2014;2(7):1707–16. https://doi.org/10.1021/sc500175v.
12. Makama S, Peters R, Undas A, van den Brink NW. A novel method for the quantification, characterisation and speciation of silver nanoparticles in earthworms exposed in soil. Environ Chem. 2015;12(6):643. https://doi.org/10.1071/en15006.
13. Jiménez-Lamana J, Abad-Álvaro I, Bierla K, Laborda F, Szpunar J, Lobinski R. Detection and characterization of biogenic selenium nanoparticles in selenium-rich yeast by single particle ICPMS. J Anal At Spectrom. 2018;33(3):452–60. https://doi.org/10.1039/c7ja00378a.
14. Mortimer M, Gogos A, Bartolomé N, Kahru A, Bucheli TD, Slaveykova VI. Potential of hyperspectral imaging microscopy for semi-quantitative analysis of nanoparticle uptake by protozoa. Environ Sci Technol. 2014;48(15):8760–7. https://doi.org/10.1021/es500898j.
15. Meyer JN, Lord CA, Yang XY, Turner EA, Badireddy AR, Marinakos SM, et al. Intracellular uptake and associated toxicity of silver nanoparticles in Caenorhabditis elegans. Aquat Toxicol. 2010;100(2):140–50. https://doi.org/10.1016/j.aquatox.2010.07.016.
16. Théoret T, Wilkinson KJ. Evaluation of enhanced darkfield microscopy and hyperspectral analysis to analyse the fate of silver nanoparticles in wastewaters. Anal Methods. 2017;9(26):3920–8. https://doi.org/10.1039/c7ay00615b.

17. Vidmar J, Loeschner K, Correia M, Larsen EH, Manser P, Wichser A, et al. Translocation of silver nanoparticles in the ex vivo human placenta perfusion model characterized by single particle ICP-MS. Nanoscale. 2018;10(25):11980–91. https://doi.org/10.1039/c8nr02096e.
18. Pena MDPS, Gottipati A, Tahiliani S, Neu-Baker NM, Frame MD, Friedman AJ, et al. Hyperspectral imaging of nanoparticles in biological samples: simultaneous visualization and elemental identification. Microsc Res Tech. 2016;79(5):349–58.
19. Brar SK, Verma M. Measurement of nanoparticles by light-scattering techniques. Trends Anal Chem. 2011;30(1):4–17. https://doi.org/10.1016/j.trac.2010.08.008.
20. Tiede K, Boxall ABA, Tear SP, Lewis J, David H, Hassellöv M. Detection and characterization of engineered nanoparticles in food and the environment. Food Addit Contam Part A. 2008;25(7):795–821. https://doi.org/10.1080/02652030802007553.
21. Correia M, Loeschner K. Detection of nanoplastics in food by asymmetric flow field-flow fractionation coupled to multi-angle light scattering: possibilities, challenges and analytical limitations. Anal Bioanal Chem. 2018;410(22):5603–15. https://doi.org/10.1007/s00216-018-0919-8.
22. Deering CE, Tadjiki S, Assemi S, Miller JD, Yost GS, Veranth JM. A novel method to detect unlabeled inorganic nanoparticles and submicron particles in tissue by sedimentation field-flow fractionation. Part Fibre Toxicol. 2008;5(1):18. https://doi.org/10.1186/1743-8977-5-18.
23. Degueldre C, Favarger PY. Colloid analysis by single particle inductively coupled plasma-mass spectroscopy: a feasibility study. Colloids Surf A Physicochem Eng Asp. 2003;217(1–3):137–42. https://doi.org/10.1016/s0927-7757(02)00568-x.
24. Olesik JW, Gray PJ. Considerations for measurement of individual nanoparticles or microparticles by ICP-MS: determination of the number of particles and the analyte mass in each particle. J Anal At Spectrom. 2012;27(7):1143. https://doi.org/10.1039/c2ja30073g.
25. Naasz S, Weigel S, Borovinskaya O, Serva A, Cascio C, Undas AK, et al. Multi-element analysis of single nanoparticles by ICP-MS using quadrupole and time-of-flight technologies. J Anal At Spectrom. 2018;33(5):835–45. https://doi.org/10.1039/c7ja00399d.
26. Shigeta K, Koellensperger G, Rampler E, Traub H, Rottmann L, Panne U, et al. Sample introduction of single selenized yeast cells (Saccharomyces cerevisiae) by micro droplet generation into an ICP-sector field mass spectrometer for label-free detection of trace elements. J Anal At Spectrom. 2013;28(5):637. https://doi.org/10.1039/c3ja30370e.
27. Walder AJ, Freedman PA. Communication. Isotopic ratio measurement using a double focusing magnetic sector mass analyser with an inductively coupled plasma as an ion source. J Anal At Spectrom. 1992;7(3):571. https://doi.org/10.1039/ja9920700571.
28. Yang L. Accurate and precise determination of isotopic ratios by MC-ICP-MS: a review. Mass Spectrom Rev. 2009;28(6):990–1011. https://doi.org/10.1002/mas.20251.
29. Tanner M, Günther D. Short transient signals, a challenge for inductively coupled plasma mass spectrometry, a review. Anal Chim Acta. 2009;633(1):19–28. https://doi.org/10.1016/j.aca.2008.11.041.
30. Borovinskaya O, Hattendorf B, Tanner M, Gschwind S, Günther D. A prototype of a new inductively coupled plasma time-of-flight mass spectrometer providing temporally resolved, multi-element detection of short signals generated by single particles and droplets. J Anal At Spectrom. 2013;28(2):226–33. https://doi.org/10.1039/c2ja30227f.
31. Guilhaus M, Selby D, Mlynski V. Orthogonal acceleration time-of-flight mass spectrometry. Mass Spectrom Rev. 2000;19(2):65–107. https://doi.org/10.1002/(sici)1098-2787(2000)19:2<65::aid-mas1>3.0.co;2-e.
32. Bandura DR, Baranov VI, Ornatsky OI, Antonov A, Kinach R, Lou X, et al. Mass cytometry: technique for real time single cell multitarget immunoassay based on inductively coupled plasma time-of-flight mass spectrometry. Anal Chem. 2009;81(16):6813–22. https://doi.org/10.1021/ac901049w.
33. Schimpf ME, Caldwell K, Giddings JC. Field-flow fractionation handbook. 2000; John Wiley & Sons
34. Shard AG, Sparnacci K, Sikora A, Wright L, Bartczak D, Goenaga-Infante H, et al. Measuring the relative concentration of particle populations using differential centrifugal sedimentation. Anal Methods. 2018;10(22):2647–57. https://doi.org/10.1039/c8ay00491a.
35. Hawkins A, Bednar AJ, Cizdziel J, Bu K, Steevens JA, Willett KL. Identification of silver nanoparticles in Pimephales promelas gastrointestinal tract and gill tissues using flow field flow fractionation ICP-MS. RSC Adv. 2014;4(78):41277–80.
36. Loeschner K, Navratilova J, Grombe R, Linsinger TPJ, Købler C, Mølhave K, et al. In-house validation of a method for determination of silver nanoparticles in chicken meat based on asymmetric flow field-flow fractionation and inductively coupled plasma mass spectrometric detection. Food Chem. 2015;181:78–84. https://doi.org/10.1016/j.foodchem.2015.02.033.
37. Loeschner K, Navratilova J, Købler C, Mølhave K, Wagner S, von der Kammer F, et al. Detection and characterization of silver nanoparticles in chicken meat by asymmetric flow field flow fractionation with detection by conventional or single particle ICP-MS. Anal Bioanal Chem. 2013;405(25):8185–95. https://doi.org/10.1007/s00216-013-7228-z.
38. Heroult J, Nischwitz V, Bartczak D, Goenaga-Infante H. The potential of asymmetric flow field-flow fractionation hyphenated to multiple detectors for the quantification and size estimation of silica nanoparticles in a food matrix. Anal Bioanal Chem. 2014;406(16):3919–27. https://doi.org/10.1007/s00216-014-7831-7.
39. Bartczak D, Vincent P, Goenaga-Infante H. Determination of size- and number-based concentration of silica nanoparticles in a complex biological matrix by online techniques. Anal Chem. 2015;87(11):5482–5. https://doi.org/10.1021/acs.analchem.5b01052.
40. Pitkänen L, Striegel AM. Size-exclusion chromatography of metal nanoparticles and quantum dots. Trends Anal Chem. 2016;80:311–20. https://doi.org/10.1016/j.trac.2015.06.013.
41. Brewer AK, Striegel AM. Particle size characterization by quadruple-detector hydrodynamic chromatography. Anal Bioanal Chem. 2008;393(1):295–302. https://doi.org/10.1007/s00216-008-2319-y.
42. Proulx K, Hadioui M, Wilkinson KJ. Separation, detection and characterization of nanomaterials in municipal wastewaters using hydrodynamic chromatography coupled to ICPMS and single particle ICPMS. Anal Bioanal Chem. 2016;408(19):5147–55. https://doi.org/10.1007/s00216-016-9451-x.
43. Lombi E, Scheckel KG, Kempson IM. In situ analysis of metal(-loid)s in plants: state of the art and artefacts. Environ Exp Bot. 2011;72(1):3–17. https://doi.org/10.1016/j.envexpbot.2010.04.005.
44. Veith L, Dietrich D, Vennemann A, Breitenstein D, Engelhard C, Karst U, et al. Combination of micro X-ray fluorescence spectroscopy and time-of-flight secondary ion mass spectrometry imaging for the marker-free detection of CeO 2 nanoparticles in tissue sections. J Anal At Spectrom. 2018;33(3):491–501.
45. Servin AD, Castillo-Michel H, Hernandez-Viezcas JA, De Nolf W, De La Torre-Roche R, Pagano L, et al. Bioaccumulation of CeO2 nanoparticles by earthworms in biochar-amended soil: a synchrotron microspectroscopy study. J Agric Food Chem. 2018;66(26):6609-6618. https://doi.org/10.1021/acs.jafc.7b04612.

46. Da Silva GH, Clemente Z, Khan LU, Coa F, Neto LL, Carvalho HW, et al. Toxicity assessment of TiO2-MWCNT nanohybrid material with enhanced photocatalytic activity on Danio rerio (Zebrafish) embryos. Ecotoxicol Environ Saf. 2018;165:136–43.
47. Mahmoud NN, Harfouche M, Alkilany AM, Al-Bakri AG, El-Qirem RA, Shraim SA, et al. Synchrotron-based X-ray fluorescence study of gold nanorods and skin elements distribution into excised human skin layers. Colloids Surf B: Biointerfaces. 2018;165:118–26.
48. Andrews JC, Meirer F, Liu Y, Mester Z, Pianetta P. Transmission X-ray microscopy for full-field nano imaging of biomaterials. Microsc Res Tech. 2011;74(7):671–81. https://doi.org/10.1002/jemt.20907.
49. Liu Y, Andrews J, Meirer F, Mehta A, Gil SC, Sciau P et al. editors. Applications of Hard X-ray Full-Field Transmission X-ray Microscopy at SSRL. In: AIP Conf Proc. AIP; 2011.
50. McRae R, Bagchi P, Sumalekshmy S, Fahrni CJ. In situ imaging of metals in cells and tissues. Chem Rev. 2009;109(10):4780–827. https://doi.org/10.1021/cr900223a.
51. ISO. International Organization for Standardization (ISO), ISO Guide 34. Geneva: General requirements for the competence of reference material producers; 2009.
52. Grombe R, Charoud-Got J, Emteborg H, Linsinger TPJ, Seghers J, Wagner S, et al. Production of reference materials for the detection and size determination of silica nanoparticles in tomato soup. Anal Bioanal Chem. 2014. https://doi.org/10.1007/s00216-013-7554-1.
53. Arslan Z, Ates M, McDuffy W, Agachan MS, Farah IO, Yu WW, et al. Probing metabolic stability of CdSe nanoparticles: alkaline extraction of free cadmium from liver and kidney samples of rats exposed to CdSe nanoparticles. J Hazard Mater. 2011. https://doi.org/10.1016/j.jhazmat.2011.05.003.
54. Loeschner K, Brabrand MSJ, Sloth JJ, Larsen EH. Use of alkaline or enzymatic sample pretreatment prior to characterization of gold nanoparticles in animal tissue by single-particle ICPMS. Anal Bioanal Chem. 2013;406(16):3845–51. https://doi.org/10.1007/s00216-013-7431-y.
55. Jiménez-Lamana J, Laborda F, Bolea E, Abad-Álvaro I, Castillo JR, Bianga J, et al. An insight into silver nanoparticles bioavailability in rats. Metallomics. 2014;6(12):2242–9. https://doi.org/10.1039/c4mt00200h.
56. Bolea E, Jiménez-Lamana J, Laborda F, Abad-Álvaro I, Bladé C, Arola L, et al. Detection and characterization of silver nanoparticles and dissolved species of silver in culture medium and cells by AsFlFFF-UV-Vis-ICPMS: application to nanotoxicity tests. Analyst. 2014;139(5):914–22. https://doi.org/10.1039/c3an01443f.
57. Klingberg H, Oddershede LB, Loeschner K, Larsen EH, Loft S, Møller P. Uptake of gold nanoparticles in primary human endothelial cells. Toxicol Res. 2015;4(3):655–66. https://doi.org/10.1039/c4tx00061g.
58. Campbell P, Ma S, Schmalzried T, Amstutz HC. Tissue digestion for wear debris particle isolation. J Biomed Mater Res. 1994;28(4):523–6. https://doi.org/10.1002/jbm.820280415.
59. Baxter RM, Steinbeck MJ, Tipper JL, Parvizi J, Marcolongo M, Kurtz SM. Comparison of periprosthetic tissue digestion methods for ultra-high molecular weight polyethylene wear debris extraction. J Biomed Mater Res B Appl Biomater. 2009;91B(1):409–18. https://doi.org/10.1002/jbm.b.31416.
60. Vidmar J, Buerki-Thurnherr T, Loeschner K. Comparison of the suitability of alkaline or enzymatic sample pre-treatment for characterization of silver nanoparticles in human tissue by single particle ICP-MS. J Anal At Spectrom. 2018;33(5):752–61. https://doi.org/10.1039/c7ja00402h.
61. Gray EP, Coleman JG, Bednar AJ, Kennedy AJ, Ranville JF, Higgins CP. Extraction and analysis of silver and gold nanoparticles from biological tissues using single particle inductively coupled plasma mass spectrometry. Environ Sci Technol. 2013;47(24):14315–23. https://doi.org/10.1021/es403558c.
62. Gajdosechova Z, Lawan MM, Urgast DS, Raab A, Scheckel KG, Lombi E, et al. In vivo formation of natural HgSe nanoparticles in the liver and brain of pilot whales. Sci Rep. 2016;6:34361. https://doi.org/10.1038/srep34361.
63. van der Zande M, Vandebriel RJ, Van Doren E, Kramer E, Herrera Rivera Z, Serrano-Rojero CS, et al. Distribution, elimination, and toxicity of silver nanoparticles and silver ions in rats after 28-day oral exposure. ACS Nano. 2012;6(8):7427–42. https://doi.org/10.1021/nn302649p.
64. Peters R, Herrera-Rivera Z, Undas A, van der Lee M, Marvin H, Bouwmeester H, et al. Single particle ICP-MS combined with a data evaluation tool as a routine technique for the analysis of nanoparticles in complex matrices. J Anal At Spectrom. 2015;30(6):1274–85. https://doi.org/10.1039/c4ja00357h.
65. Peters RJB, Rivera ZH, van Bemmel G, Marvin HJP, Weigel S, Bouwmeester H. Development and validation of single particle ICP-MS for sizing and quantitative determination of nano-silver in chicken meat. Anal Bioanal Chem. 2014. https://doi.org/10.1007/s00216-013-7571-0.
66. Schmidt B, Loeschner K, Hadrup N, Mortensen A, Sloth JJ, Bender Koch C, et al. Quantitative characterization of gold nanoparticles by field-flow fractionation coupled online with light scattering detection and inductively coupled plasma mass spectrometry. Anal Chem. 2011;83(7):2461–8. https://doi.org/10.1021/ac102545e.
67. Hadioui M, Peyrot C, Wilkinson KJ. Improvements to single particle ICPMS by the online coupling of ion exchange resins. Anal Chem. 2014;86(10):4668–74. https://doi.org/10.1021/ac5004932.
68. Heringa MB, Peters RJB, Bleys RLAW, van der Lee MK, Tromp PC, van Kesteren PCE, et al. Detection of titanium particles in human liver and spleen and possible health implications. Part Fibre Toxicol. 2018;15(1). https://doi.org/10.1186/s12989-018-0251-7.
69. Peters RJB, van Bemmel G, Herrera-Rivera Z, Helsper HPFG, Marvin HJP, Weigel S, et al. Characterization of titanium dioxide nanoparticles in food products: analytical methods to define nanoparticles. J Agric Food Chem. 2014;62(27):6285–93. https://doi.org/10.1021/jf5011885.
70. Modrzynska J, Berthing T, Ravn-Haren G, Kling K, Mortensen A, Rasmussen RR, et al. In vivo-induced size transformation of cerium oxide nanoparticles in both lung and liver does not affect long-term hepatic accumulation following pulmonary exposure. PLoS One. 2018;13(8):e0202477. https://doi.org/10.1371/journal.pone.0202477.
71. Graham UM, Tseng MT, Jasinski JB, Yokel RA, Unrine JM, Davis BH, et al. In vivo processing of ceria nanoparticles inside liver: impact on free-radical scavenging activity and oxidative stress. Chem Aust. 2014;79(8):1083–8. https://doi.org/10.1002/cplu.201402080.
72. Yamashita K, Yoshioka Y, Higashisaka K, Mimura K, Morishita Y, Nozaki M, et al. Silica and titanium dioxide nanoparticles cause pregnancy complications in mice. Nat Nanotechnol. 2011;6(5):321–8. https://doi.org/10.1038/nnano.2011.41.
73. Pietroiusti A, Massimiani M, Fenoglio I, Colonna M, Valentini F, Palleschi G, et al. Low doses of pristine and oxidized single-wall carbon nanotubes affect mammalian embryonic development. ACS Nano. 2011;5(6):4624–33. https://doi.org/10.1021/nn200372g.
74. Campagnolo L, Massimiani M, Palmieri G, Bernardini R, Sacchetti C, Bergamaschi A, et al. Biodistribution and toxicity of pegylated single wall carbon nanotubes in pregnant mice. Part Fibre Toxicol. 2013;10(1):21. https://doi.org/10.1186/1743-8977-10-21.
75. Hougaard KS, Campagnolo L, Chavatte-Palmer P, Tarrade A, Rousseau-Ralliard D, Valentino S, et al. A perspective on the developmental toxicity of inhaled nanoparticles. Reprod Toxicol. 2015;56:118–40. https://doi.org/10.1016/j.reprotox.2015.05.015.
76. Drescher D, Giesen C, Traub H, Panne U, Kneipp J, Jakubowski N. Quantitative imaging of gold and silver nanoparticles in single

eukaryotic cells by laser ablation ICP-MS. Anal Chem. 2012;84(22):9684–8. https://doi.org/10.1021/ac302639c.
77. Koeman JH, van de Ven WSM, de Goeij JJM, Tjioe PS, van Haaften JL. Mercury and selenium in marine mammals and birds. Sci Total Environ. 1975;3(3):279–87. https://doi.org/10.1016/0048-9697(75)90052-2.
78. Tuoriniemi J, Cornelis G, Hassellöv M. Size discrimination and detection capabilities of single-particle ICPMS for environmental analysis of silver nanoparticles. Anal Chem. 2012;84(9):3965–72. https://doi.org/10.1021/ac203005r.
79. Tuoriniemi J, Cornelis G, Hassellöv M. Improving the accuracy of single particle ICPMS for measurement of size distributions and number concentrations of nanoparticles by determining analyte partitioning during nebulisation. J Anal At Spectrom. 2014;29(4):743–52. https://doi.org/10.1039/c3ja50367d.
80. Gschwind S, Aja Montes ML, Günther D. Comparison of sp-ICP-MS and MDG-ICP-MS for the determination of particle number concentration. Anal Bioanal Chem. 2015;407(14):4035–44. https://doi.org/10.1007/s00216-015-8620-7.
81. Yin R, Feng X, Meng B. Stable mercury isotope variation in rice plants (Oryza sativa L.) from the Wanshan Mercury Mining District, SW China. Environ Sci Technol. 2013;47(5):2238–45. https://doi.org/10.1021/es304302a.
82. Nuñez J, Renslow R, Cliff JB, Anderton CR. NanoSIMS for biological applications: current practices and analyses. Biointerphases. 2018;13(3):03B301. https://doi.org/10.1116/1.4993628.
83. Georgantzopoulou A, Serchi T, Cambier S, Leclercq CC, Renaut J, Shao J, et al. Effects of silver nanoparticles and ions on a co-culture model for the gastrointestinal epithelium. Part Fibre Toxicol. 2016;13(1). https://doi.org/10.1186/s12989-016-0117-9.
84. Mehennaoui K, Georgantzopoulou A, Felten V, Andreï J, Garaud M, Cambier S, et al. Gammarus fossarum (Crustacea, Amphipoda) as a model organism to study the effects of silver nanoparticles. Sci Total Environ. 2016;566-567:1649–59. https://doi.org/10.1016/j.scitotenv.2016.06.068.
85. Henss A, Otto S-K, Schaepe K, Pauksch L, Lips KS, Rohnke M. High resolution imaging and 3D analysis of Ag nanoparticles in cells with ToF-SIMS and delayed extraction. Biointerphases. 2018;13(3):03B410. https://doi.org/10.1116/1.5015957.
86. Lopes VR, Loitto V, Audinot J-N, Bayat N, Gutleb AC, Cristobal S. Dose-dependent autophagic effect of titanium dioxide nanoparticles in human HaCaT cells at non-cytotoxic levels. J Nanobiotechnol. 2016;14(1). https://doi.org/10.1186/s12951-016-0174-0.
87. Bettini S, Boutet-Robinet E, Cartier C, Coméra C, Gaultier E, Dupuy J, et al. Food-grade TiO2 impairs intestinal and systemic immune homeostasis, initiates preneoplastic lesions and promotes aberrant crypt development in the rat colon. Sci Rep. 2017;7(1). https://doi.org/10.1038/srep40373.
88. Yang Y-SS, Atukorale PU, Moynihan KD, Bekdemir A, Rakhra K, Tang L, et al. High-throughput quantitation of inorganic nanoparticle biodistribution at the single-cell level using mass cytometry. Nat Commun. 2017;8:14069. https://doi.org/10.1038/ncomms14069.
89. Ivask A, Mitchell AJ, Hope CM, Barry SC, Lombi E, Voelcker NH. Single cell level quantification of nanoparticle–cell interactions using mass cytometry. Anal Chem. 2017;89(16):8228–32. https://doi.org/10.1021/acs.analchem.7b01006.